Solar Energy Materials & Solar Cells 262 (2023) 112555

Contents lists available at ScienceDirect

Solar Energy Materials and Solar Cells

journal homepage: www.elsevier.com/locate/solmat

Theoretical analysis of backside polycrystalline silicon layer in the TOPCon solar cells

Mengchao Du [a,b,c], Rui Jia [b,c,*], Xing Li [b,c,**], Xinhe Zheng [a,***], Zhibo Gao [b,c], Jiawang Chen [b,c], Peng Qiu [a], Heng Liu [a], Jin Yang [a], Delin Kong [a]

[a] School of Mathematics and Physics, Beijing Key Laboratory for Magneto-Photoelectrical Composite and Interface Science, University of Science and Technology Beijing, Beijing, 100083, China
[b] Institute of Microelectronics of the Chinese Academy of Sciences, Beijing, 100029, China
[c] University of Chinese Academy of Sciences, Beijing, 100029, China

ARTICLE INFO

Keywords:
TOPCon
Poly-Si
Band gap
Defect states

ABSTRACT

As an upgraded version of passivated emitter and rear cell (PERC) solar cells, the performance of tunnel oxide passivating contacts (TOPCon) solar cells is very dependent on the silicon oxide layer and poly-Si layer. We found that different crystallization rates or doping of germanium, carbon and other elements in poly-Si can change the band gap of poly-Si, which has an impact on the efficiency (E_{ff}) of TOPCon solar cells. Therefore, the appropriate band gap is particularly important. At the same time, the internal defect of poly-Si also have great influence on the performance of solar cells. The simulated band diagram, charge carrier concentration and recombination rate were used to deeply explore the defect in poly-Si and the influence of poly-Si with different band gap on the performance of TOPCon solar cells.

1. Introduction

For crystalline silicon solar cells, the key to improving E_{ff} is to reduce the recombination loss between silicon and electrode. The quality of passivation has a decisive impact on the quality of the cell, and it can even be said that the development of cell technology can be attributed to the development of passivation technology [1]. In 2013, the Frauhofor Institute in Germany introduced the TOPCon technology concept [2]. As one of the solar cells with the best passivation performance, the TOPCon solar cell using N-type silicon as substrate has achieved an impressive open-circuit voltage (V_{oc}) of 703 mV and E_{ff} of 23.7% at the very beginning of its introduction. This has shown its wide development space and potential. Since then, TOPCon solar cells have received more attention. In 2016, the Georgia Institute of Technology [3] achieved 21.2% of conversion E_{ff}. In June 2016, Hamelin Solar Energy Research Institute (ISFH) [4] increases the V_{oc} of TOPCon structure to 748 mV and the lowest dark saturation current density reached 0.6 fA/cm^2 by annealing doped amorphous silicon prepared by low pressure chemical vapor deposition (LPCVD). In 2018 [5], TOPCon solar cells with an E_{ff} of up to 25.7% were successfully prepared. On November 19, 2022, Martin Green announced via video that Longi Green Energy Technology Co.,ltd. 26.81% cell E_{ff} is currently the highest record for silicon solar cell E_{ff} in the world.

From a commercial point of view, it is currently estimated that silicon-based solar cells account for more than 90% of the PV market. Among the many silicon solar cells, PERC solar cells, as the mainstream, occupy a larger market on the one hand, on the other hand, PERC cell efficiency is close to the theoretical limit. At present, the solar cells that are expected to succeed PERC cells as the mainstream are mainly Heterojunction with Intrinsic Thin-film (HJT) [6,7], TOPCon and Interdigitated Back Contact (IBC). Thanks to the double passivation effect of n-type silicon substrate and substrate surface defect, the efficiency of HJT has been greatly improved at present. It is reported that HJT efficiency has reached an amazing 26.81%. As the substrate is phosphorus-doped n-type single crystal silicon, there is no boron-oxygen recombination or boron-iron recombination in p-type crystalline silicon,

* Corresponding author. Institute of Microelectronics of the Chinese Academy of Sciences, Beijing, 100029, China.
** Corresponding author. Institute of Microelectronics of the Chinese Academy of Sciences, Beijing, 100029, China.
*** Corresponding author. School of Mathematics and Physics, Beijing Key Laboratory for Magneto-Photoelectrical Composite and Interface Science, University of Science and Technology Beijing, Beijing, 100083, China.
E-mail addresses: jiarui@ime.ac.cn (R. Jia), lixing2021@ime.ac.cn (X. Li), xinhezheng@ustb.edu.cn (X. Zheng).

https://doi.org/10.1016/j.solmat.2023.112555
Received 18 July 2023; Received in revised form 31 August 2023; Accepted 8 September 2023
Available online 23 September 2023

etc., so there is no light induced degradation (LID) effect in HJT [8]. The absence of an insulating layer on the surface also makes it possible to avoid the potential induced degradation (PID) effect. Currently, Liu et al. [9] have successfully developed flexible HJT solar cells. Through the low-temperature process and symmetric design, the wafer's thickness was greatly reduced but the good surface passivation was well kept. However, due to the high investment in equipment and manufacturing costs, the development of HJT is relatively slow. Compared with other solar cells, IBC benefit from their structure with higher fill factor (*FF*) and short-circuit current density (J_{sc}). However, the cost is almost twice that of conventional cells. Compared to HJT and IBC, TOPCon solar cells have a unique advantage in terms of manufacturing process, which is highly compatible with PERC cells, requiring only additional boron diffusion equipment and tunneling layer and poly-Si deposition equipment. This greatly reduces the cost of solar cells iterations. Therefore, considerations from an economic point of view, the commercialization of TOPCon solar cells has great advantages.

Compared with the mainstream solar cell technologies such as PERC and HJT, TOPCon solar cells use a tunneling layer on the back side to reduce the carrier recombination between the metal electrode and silicon. Since the tunneling potential of the tunneling oxide layer for holes (4.5 eV) is higher than that of electrons (3.1 eV), it is easier for electrons to tunnel and be collected. Another function of the tunneling oxide layer is full-area passivation, and the excellent passivation ability further improves the efficiency of TOPCon solar cells. Compared to PERC, TOPCon solar cells are one-dimensional carrier transport structure carriers can be efficiently transported longitudinally through the oxide layer in one dimension [10,11]. Avoiding recombination during transmission reduces series resistance and improves solar cells *FF*. Therefore, as the core process of TOPCon solar cells, the backside oxide layer and poly-Si layer have always been the focus of research on TOPCon solar cells [12–14].

Unfortunately, there is no perfect explanation of the carrier transport mechanism in the highly doped poly-Si/silicon oxide/monocrystalline silicon structure. It is found that both the silicon oxide layer and the poly-Si layer have an influence on the passivation contact effect, and only when the two structures are better matched together can the desired passivation effect be achieved [15,16]. According to the study, it is known that there is a pinhole structure in the silicon oxide, which has an auxiliary role in carrier transport and even plays a dominant role at higher pinhole densities. In addition to the pinhole structure, on the surface of silicon oxide, there exists a kind of subnanometer pits. According to Liu et al. [17], these subnanometer pits provide excellent surface passivation and efficient tunneling for majority carriers. As a unique and very important structure of TOPCon, the poly-Si layer has a very important influence on TOPCon solar cells, and the main role of poly-Si is speculated to be passivation.

2. Simulation structure for TOPCon solar cell

The structure of TOPCon solar cells used for simulation is shown in Fig. 1. The front emitting layer on the front side of the model is in thermal diffusion contact with the substrate, while the contact between the substrate and the back field layer is a tunneling oxide passivation contact with ultrathin silicon oxide (SiO_x)/poly-Si passivation contact. The structure of the TOPCon solar cells is a conductive oxide TCO/p^+-poly-Si/n-Si-wafer/SiO_x/n^+-poly-Si/metal [18], and the parameters of each layer are set as in Table 1. All the following parameters are corresponding to the real solar cell. At the p^+-type emitter, its thickness is 30 nm which is related to the optimized selective emitter doping profile.

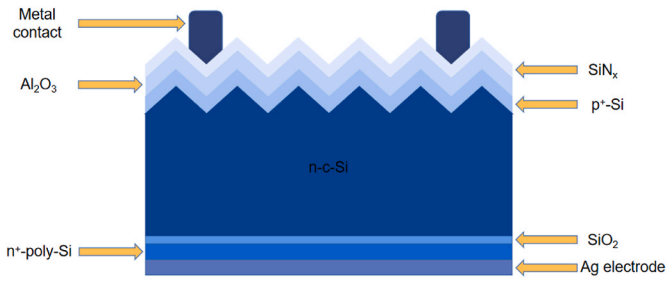

Fig. 1. Structure of TOPCon solar cells for the simulation.

The structure of poly-Si itself leads to many defect in its band gap [19]. In most of the papers [20,21], the defect distribution in poly-Si is modeled similarly. Exponentially distributed band tailed states and Gaussian distributed donor-like defect states and acceptor-like defect states. But the actual situation is often more complicated. Chen et al. [22] obtained activation energies in the range of 0.25–0.3 eV for poly-Si films prepared by plasma enhanced chemical vapor deposition (PECVD) by charge pumping method. Armstong et al. [23] similarly confirmed the trap energy level at 0.43 eV below the conduction band by deep level transient spectroscopy (DLTS) spectroscopy and the existence of several discrete energy states in the range of 0.2–0.5 eV below the conduction band. Sehil et al. [24] confirmed the existence of grain boundary defect states formed by suspended bonds at 0.40 eV below the conduction band of poly-Si thin film materials by the field effect method. Kim et al. [25] confirmed the existence of high density trap states in the center of the band gap through charge-pump measurement. This result has also been verified by several other experiments [26–29]. Jeong et al. [30] found a deep-level trap states near 0.35–0.5 eV above the valence band of the poly-Si thin film deposited by LPCVD method, and believed that it was related to the additional band-gap energy states formed near the SiO_2/poly-Si interface during laser annealing.

The poly-Si defect states in the n^+-type polysilicon layers are Gaussian distributed, as detailed in Table 2. In the Table 2, E_s is the defective energy level.

3. Results and discussion

The simulation results show that with the increase of band gap, the V_{oc}, J_{sc} and E_{ff} of solar cells are improved. The increase of defect states concentration will lead to the deterioration of solar cell performance. Among them, the acceptor-like defect states have the ability to capture electrons, so the impact on the solar cells is more obvious.

3.1. Effect of band gap width on TOPCon solar cells

In TOPCon solar cells, poly-Si layer has a great impact on the quality of the cell. Current research focuses on phosphorus doping concentration and tunneling oxide layer thickness, while often ignoring the impact of poly-Si band gap width and defect in poly-Si on TOPCon solar cells.

At present, the main manufacturing technology of poly-Si in TOPCon solar cells back field layer is LPCVD or PECVD. As to poly-Si fabricated by LPCVD, the band gap width is difficult to adjust. But by PECVD, the poly-Si's band gap width can be adjusted by high temperature annealing or doping of C and O. Under different annealing conditions, the crystallization rate of amorphous silicon films grown by PECVD is often very different, and the band gap of poly-Si is closely related to the crystallization rate of poly-Si. The higher the crystallization rate, the smaller the

Table 1
Parameters of TOPCon solar cells.

Layer	Default parameters
Front contact	Metal-Semiconductor Contacts
p^+-type Si layer	t = 30 nm, N_a = 8E19
Interface	Drift-diffusion
n-type c-Si layer	t = 140 μm, N_d = 8E16
Interface(SiO_x)	Chi = 1 eV, E_g = 8.9 eV, dk = 3.9, m_e = 0.98 m_0, m_h = 0.49 m_0
n^+-type Si layer	t = 120 nm, N_a = 2E20
Rear contact	Metal-Semiconductor Contacts
Ag electrode	t = 10 μm

Table 2
Distribution of poly-Si defect states.

trap states (E_c − E_s)/eV	Defect states concentration/ cm^{-3}	Characteristic of defect states
0.45	1E18	donor-like
0.59	1E18	donor-like
0.76	1E19	donor-like
0.24	1E18	acceptor-like

band gap of poly-Si. In addition to the crystallization rate, doping also affects the band gap of poly-Si, for example, when the amorphous silicon is doped with germanium, the amorphous silicon band gap will be decrease when doped with carbon, then the band gap will increase. With the change of band gap, V_{oc}, J_{sc}, *FF* and E_{ff} of TOPCon solar cells have been greatly changed.

Fig. 2 shows the V_{oc}, J_{sc}, *FF* and E_{ff} of TOPCon solar cells with different band gaps. By changing the band gap width from 1.11 eV to 1.34 eV, the V_{oc} of TOPCon solar cells increases from 711.6 to 745.5 mV, J_{sc} increases from 39.17 to 41.34 mA/cm^2, and *FF* increases from 79.03% to 85.20%. E_{ff} increases from 22.03% to 26.26%, and then the solar cell performance changes dramatically with increasing poly-Si band gap.

Solar cell open circuit voltage

$$V_{oc} = V_T \ln(1 + I_L / I_0) \tag{1}$$

Where the reverse saturation current

$$I_0 \propto e^{-E_g/(KT)} \tag{2}$$

From which we can learn that $V_{OC} \propto E_g$, the open circuit voltage is positively correlated with the band gap width. Consequently, the polysilicon band gap width is increased and the open circuit voltage is enhanced.

$$n = N_c \bullet exp\left(-\left(E_c - E_{fn}\right) / k_0 T\right) \tag{3}$$

$$p = N_v \bullet exp\left(-\left(E_{fp} - E_v\right) / k_0 T\right) \tag{4}$$

The equation of electron and hole concentration is shown in Eq. (3) and Eq. (4) [31]. According to the analysis of the energy band diagram under the illumination condition in Fig. 3. At the poly-Si interface, the corresponding (E_c-E_{fn}) values of the band gaps of 1.11 eV, 1.22 eV, 1.34 eV and 1.44 eV are 0.0749 eV, 0.0827 eV, 0.0794 eV and 0.0794 eV, respectively. According to Eq. (3), the electron concentration reaches its minimum when the band gap width is 1.22 eV. With the increase of the band gap width of poly-Si, the value of (E_{fp}-E_v) shows an increasing tendency and the hole concentration decreases.

According to the energy band diagram of illumination shown in Fig. 3, when the band gap of poly-Si is small, the bending of valence band at the interface between poly-Si and monocrystalline silicon will produce a quantum well(The horizontal axis in the figure represents the distance to the upper surface of p^+-type Si layer). Due to the presence of quantum wells, a large number of holes accumulate in this region. As the polysilicon band gap increases, the quantum well depth gradually decreases, and it has disappeared, when the poly-Si band gap is 1.34 eV.

Fig. 4 shows that when the band gap of poly-Si is below 1.22 eV, the electron-hole recombination is mainly concentrated on the side at the poly-Si interface. With the increase of band gap, the recombination rate decreases. When the band gap reaches 1.34 eV, the recombination region changes and shifts from the poly-Si interface to the single-crystal silicon interface, while the recombination rate decreases sharply. The recombination rate at the interface decreases by two orders of magnitude when the poly-Si band gap reaches 1.34 eV compared to the narrow band gap.

From Fig. 3, it can be seen that when the band gap is less than 1.22 eV, a triangle quantum well is formed on the poly-Si side at the interface between poly-Si and monocrystalline silicon, causing a large number of holes to concentrate. Therefore, electron-hole recombination is concentrated at the interface of poly-Si. Meanwhile, due to a large number of electron-hole recombination, the leakage current generated is large, resulting in a low *FF* of TOPCon solar cells. With the increase of the band gap, the depth of the quantum well decreases until it disappears. When the quantum well disappears, a large number of holes in the poly-Si will pour into the monocrystalline silicon, and the concentration of holes in the poly-Si at the interface becomes smaller. Therefore, when the band gap is greater than 1.34 eV, electron-hole recombination will

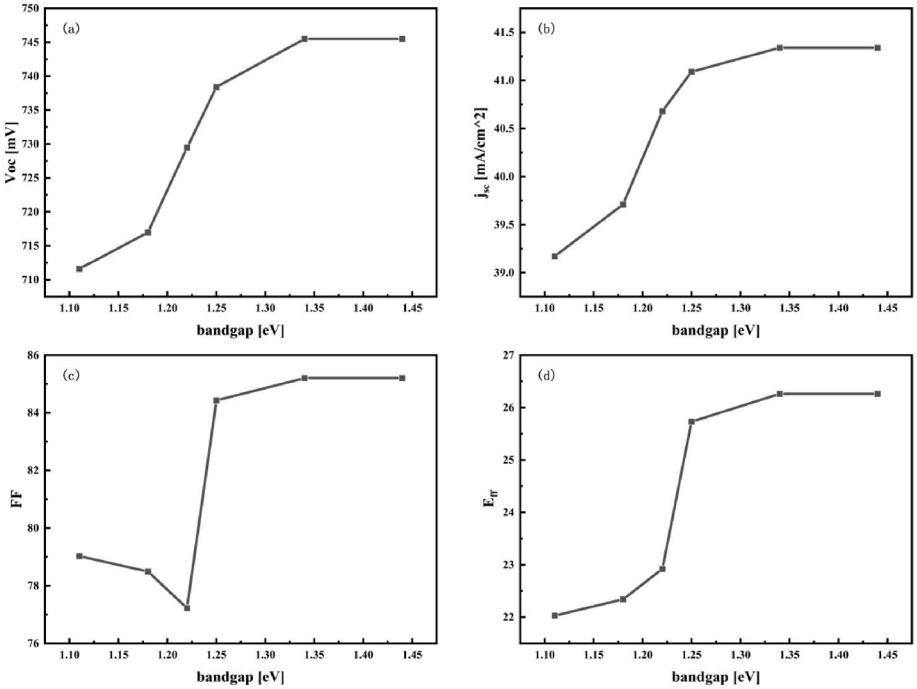

Fig. 2. Effects of band gap widths on(a) V_{oc}; (b) J_{sc}; (c) *FF*; (d) E_{ff} of the TOPCon solar cells.

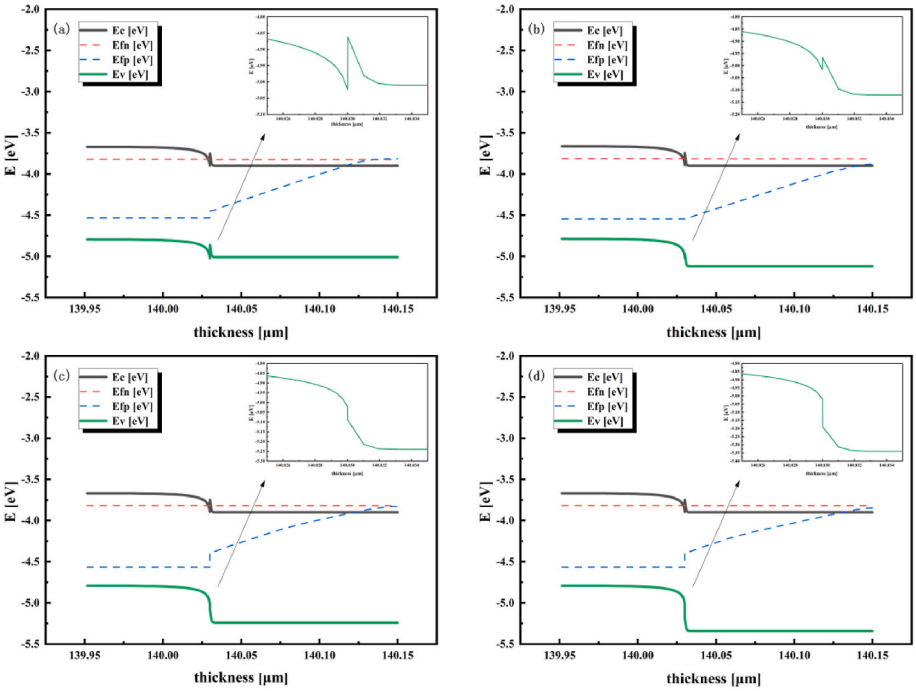

Fig. 3. The band diagram of the interface with different band gaps under light conditions (a)1.11 eV (b)1.22 eV (c)1.34 eV (d)1.44 eV.

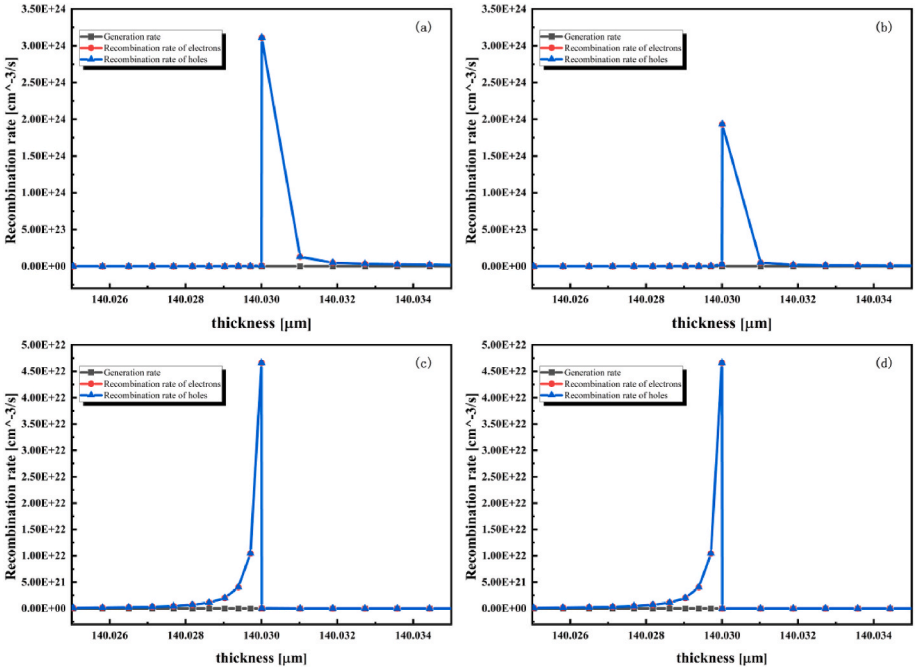

Fig. 4. Recombination rate at different band gap interfaces under light conditions (a) 1.11 eV (b) 1.22 eV (c) 1.34 eV (d) 1.44 eV.

mainly occur in monocrystalline silicon.

3.2. The effect of defect states on TOPCon solar cells

In poly-Si, the defect states include valence band band-tail localized states, conduction band band-tail localized states, and four gap states with Gaussian distribution. Band-tail localization is caused by bond Angle distortion, gap localization is caused by suspension bond. In the gap states in poly-Si can be divided into donor-like defect states and acceptor-like defect states. As the defect states concentration increases, the performance of TOPCon solar cells decreases.

Fig. 5 shows the effect of the variation of the concentration of acceptor-like defect states on the performance of TOPCon solar cells. It can be seen that the V_{oc} and J_{sc} of the TOPCon solar cells decreases continuously with the increase of the concentration of the acceptor-like defect states. However, *FF* shows an increasing trend, and E_{ff} of TOPCon solar cells becomes significantly worse with increasing concentration. The defect states concentration of acceptor-like defect states increases from 1E18 to 1.5E20, the V_{oc} of TOPCon solar cells decreases from 729.5 to 692 mV, J_{sc} decreases from 40.68 to 36.02 mA/cm^2, and *FF* increases from 77.23% to 80.95%. E_{ff} decreases from 22.92% to 20.18%. We speculate that acceptor-like defect states increase the reverse saturation

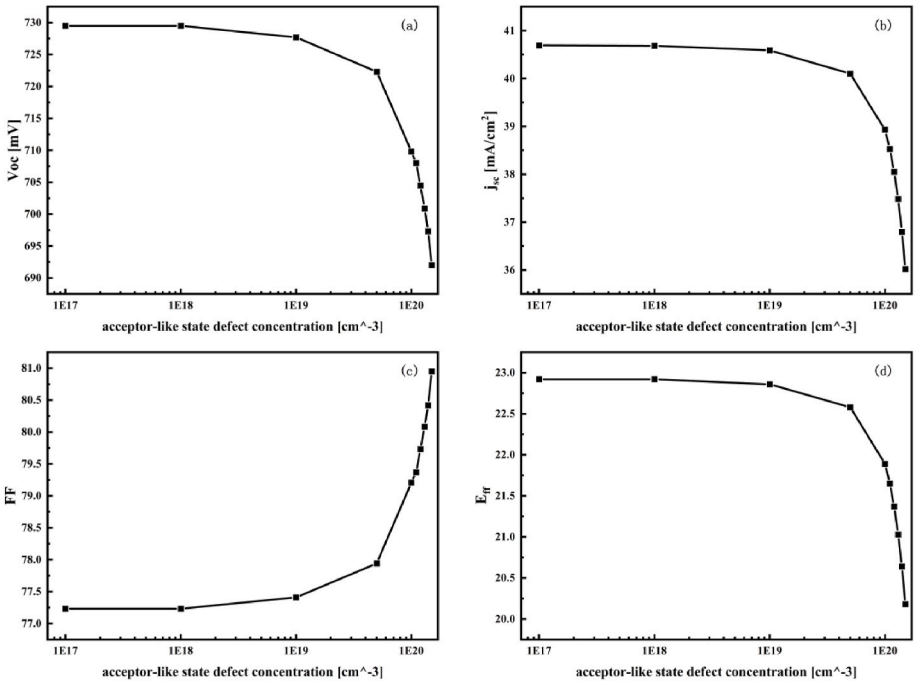

Fig. 5. Effects of acceptor-like defect states concentration on(a) V_{oc}; (b) J_{sc}; (c) *FF*; (d) E_{ff} of the TOPCon solar cells.

current, resulting in lower open-circuit voltage. Also, acceptor-like defect states affect photon absorption and carrier collection, leading to lower short-circuit current density and efficiency. However, acceptor-like defect states also reduce the surface recombination and increase the carrier lifetime, leading to an increase in the FF.

As can be seen from the poly-Si band diagram Fig. 6, when the defect states concentration of the acceptor-like defect states is high, the Fermi level will be below the conduction band. This is due to the high concentration of defect, the electrons that originally almost filled the quantum states near the bottom of the conduction band were recombined by defect. At the same time, it is found that the conduction band at the interface of monocrystalline silicon is lower than that of poly-Si, so a large number of electrons will accumulate here.

Due to the large number of electrons being recombined by the defect, a large number of quantum states near the bottom of the conduction band are released. This causes a large number of electrons in monocrystalline silicon to emission into poly-Si. In Fig. 7, it can be seen that compared to a defect states concentration of 1E18 in the acceptor-like defect states, when the acceptor-like defect states reaches 1.5E20, the electron concentration in poly-Si decreases by two energy levels, while the charge density in the defect nearly doubles. At the interface between monocrystalline silicon and poly-Si, the number of electrons on the monocrystalline silicon side is significantly reduced, which makes the recombination rate in the poly-Si region decrease.

Since there are three donor-like defect states in poly-Si, changing their defect states concentrations separately reveals that the change in defect states concentration at different locations has a consistent effect on the V_{oc}, J_{sc}, *FF* and E_{ff} of TOPCon solar cells when changing only one defect states concentration alone.The defect states concentration of donor-like defect states increases from 1E18 to 1.5E20, the V_{oc} of TOPCon solar cells decreases from 729.5 mV to 720.5 mV, the J_{sc}

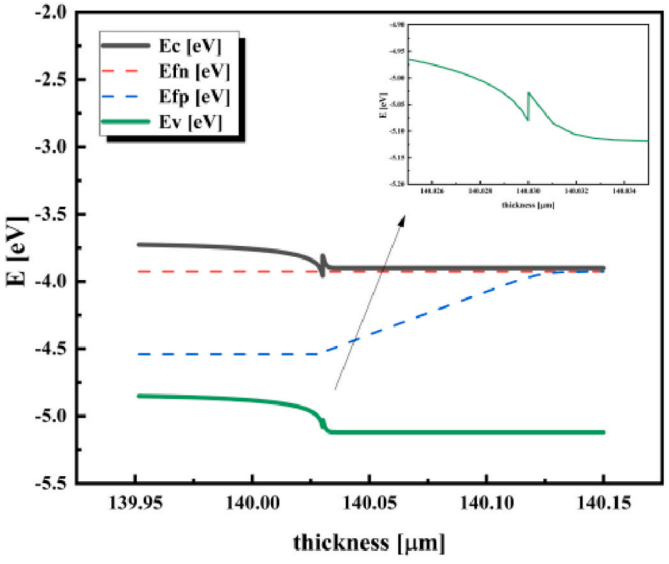

Fig. 6. The energy band diagram of acceptor-like defect states concentration of 1.5E20.

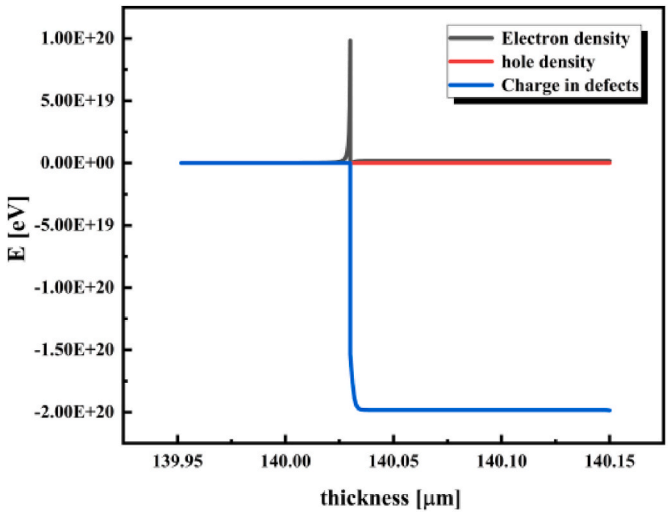

Fig. 7. Concentration of acceptor-like defect states concentration of 1.5E20.

decreases from 40.68 mA/cm^2 to 40.07 mA/cm^2, *FF* increases from 77.23% to 78.13% and E_{ff} increases from 22.22% to 22.56%. But simultaneously changing the three defect states concentrations so that the three defect states concentrations are equal and the sum of the defect states concentrations is 1.5E20 found that the V_{oc} is 720.5 mV, the J_{sc} is 40.1 mA/cm^2, the *FF* is 78.13%, and the E_{ff} is 22.58%. Compared to changing the concentration of the donor-like defect states at a single location, changing all three defect simultaneously results in no change in V_{oc} and *FF*, and only a small increase in J_{sc}, which leads to the increase in TOPCon solar cells E_{ff}. This is because the donor-like defect states are distributed near the center of the forbidden zone and the energy difference between them is small. Therefore, changing the concentration of all three defect at the same time is not much different from changing one of the defect alone.

It can be found that TOPCon solar cells are more sensitive to the change of defect states concentration of the acceptor-like defect states. When the defect states concentration of the acceptor-like defect states is less than one order of magnitude of doping concentration, the cell E_{ff} decreases rapidly with the increase of defect states concentration.

Compared with the acceptor-like defect states, the donor-like defect states have much less impact on TOPCon solar cells. The recombination rate at the interface of poly-Si increases with the increase of donor-like defect states concentration. As can be seen from the poly-Si band diagram Fig. 8, a large number of holes accumulate at the poly-Si interface due to the existence of triangle quantum well, and the increase of donor-like defect states concentration will lead to the increase of recombination.

In addition to exploring the effect of the concentration of donor-like defect states on the performance of solar cells, the effect of different positions of the donor-like defect states on the performance of TOPCon solar cells. It is finally found that the effects of donor-like defect states at different locations on the performance of TOPCon solar cells are not significantly different. This is probably because all the donor-like defect states are concentrated in the middle of the band gap, so the defect have a similar effect on the device mechanism. The difference between changing the concentration of defect states in all donor-like defect states at the same time and changing the concentration of defect states in one of them is only the difference in the total number of defect in donor-like defect states. However, in TOPCon solar cells, the influence of defect states concentration of the same order of magnitude on the cells is almost the same.

4. Conclusions

The poly-Si on the back has a great impact on the performance of TOPCon solar cells. In the case of narrow band system, the quantum well formed at the valence band at the interface of poly-Si leads to the accumulation of holes, which makes the recombination rate surge and leads to poor device performance. When the band gap increases to 1.34 eV, the quantum well disappears, the recombination rate decreases by two orders of magnitude, and the performance improves. Therefore, in order to obtain good TOPCon solar cells, attention should be paid to control the width of the band gap when preparing poly-Si layers. At the same time, we should be careful of reducing the defect states concentration in the poly-Si layer, especially in the acceptor-like defect states. It should be controlled to less than 1-2 orders of magnitude doping concentration.

CRediT authorship contribution statement

Mengchao Du: Writing – review & editing, Writing – original draft, Validation, Software, Resources, Methodology, Investigation, Formal analysis, Data curation. **Rui Jia:** Writing – review & editing, Supervision, Funding acquisition. **Xing Li:** Supervision. **Xinhe Zheng:** Writing – review & editing, Supervision. **Zhibo Gao:** Supervision, Software. **Jiawang Chen:** Supervision. **Peng Qiu:** Supervision, Software. **Heng Liu:** Supervision. **Jin Yang:** Supervision, Software. **Delin Kong:** Software.

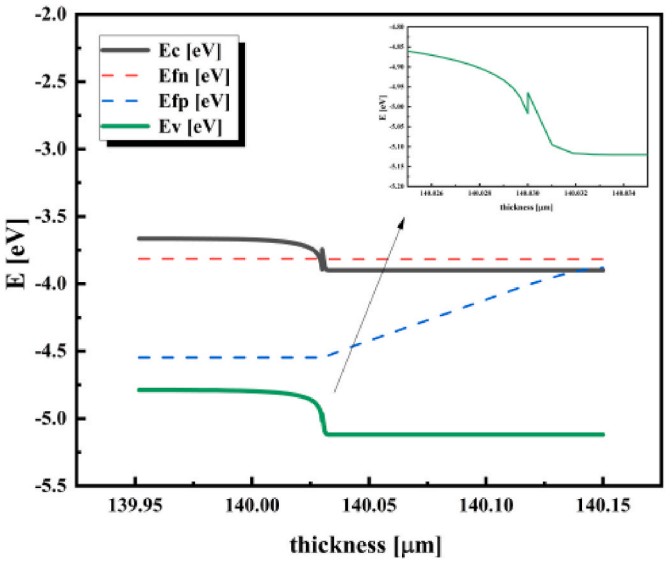

Fig. 8. The band diagram of donor-like defect states concentration of 1.5E20.

Declaration of competing interest

The authors declare that they have no known competing financial interests or personal relationships that could have appeared to influence the work reported in this paper.

Data availability

No data was used for the research described in the article.

Acknowledgements

This work was supported by the National Key Research and Development Program of China (2022YFF0709500, 2020YFB1506503, 2018YFB1500500, 2018YFB1500200), National Natural Science Foundation of China (NSFC, Grant Nos. 12035020, 52072399, 62074165, 12175305, 62104253 and 12105357), Natural Science Foundation of Beijing Municipality (4192064, 1212015), National Key Research and Development Program of China (2018YFA0703700).

References

[1] R.S. Bonilla, et al., Dielectric surface passivation for silicon solar cells: a review, Phys. Status Solidi 214 (7) (2017), 1700293, https://doi.org/10.1002/pssa.201700293.
[2] S.W. Glunz, et al., A Passivated Rear Contact for High-Efficiency n-type Si Solar Cells Enabling High Voc's and FF>82 %, 2013, https://doi.org/10.4229/28THEUPVSEC2013-2CO.4.4.
[3] T. Yuguo, et al., Tunnel oxide passivated rear contact for large area n-type front junction silicon solar cells providing excellent carrier selectivity, AIMS Materials Science 3 (1) (2016) 180–189, https://doi.org/10.3934/matersci.2016.1.180.
[4] S. Frigge, et al., Implementation of N+ and p+ Poly Junctions on Front and Rear Side of Double-Side Contacted Industrial Silicon Solar Cells, 2016, https://doi.org/10.4229/EUPVSEC20162016-2BO.3.2.
[5] A. Richter, et al., n-Type Si solar cells with passivating electron contact: identifying sources for efficiency limitations by wafer thickness and resistivity variation, Sol. Energy Mater. Sol. Cell. 173 (2017) 96–105, https://doi.org/10.1016/j.solmat.2017.05.042.
[6] X. Ru, et al., 25.11% efficiency silicon heterojunction solar cell with low deposition rate intrinsic amorphous silicon buffer layers, Sol. Energy Mater. Sol. Cell. 215 (2020), 110643, https://doi.org/10.1016/j.solmat.2020.110643.
[7] M. Wang, et al., Influence of unintentional H2O introduction in sputtering chamber on ITO films and HJT solar cells, Sol. Energy Mater. Sol. Cell. 254 (2023), 112274, https://doi.org/10.1016/j.solmat.2023.112274.
[8] W. Liu, et al., Light-induced activation of boron doping in hydrogenated amorphous silicon for over 25% efficiency silicon solar cells, Nat. Energy 7 (5) (2022) 427–437, https://doi.org/10.1038/s41560-022-01018-5.

[9] W. Liu, et al., Flexible solar cells based on foldable silicon wafers with blunted edges, Nature 617 (7962) (2023) 717–723, https://doi.org/10.1038/s41586-023-05921-z.
[10] F. Feldmann, et al., Tunnel oxide passivated contacts as an alternative to partial rear contacts, Sol. Energy Mater. Sol. Cell. 131 (2014) 46–50, https://doi.org/10.1016/j.solmat.2014.06.015.
[11] Q. Wang, et al., Influence of SiOx film thickness on electrical performance and efficiency of TOPCon solar cells, Sol. Energy Mater. Sol. Cell. 208 (2020), 110423, https://doi.org/10.1016/j.solmat.2020.110423.
[12] N. Lin, et al., *Excellent surface passivation of p-type TOPCon enabled by ozone-gas oxidation with a single-sided saturation current density of ~ 4.5 fA/cm^2*, Sol. Energy 259 (2023) 348–355, https://doi.org/10.1016/j.solener.2023.05.028.
[13] C. Guo, et al., Influence of backside surface morphology on passivation and contact characteristics of TOPCON solar cells, Sol. Energy 258 (2023) 278–288, https://doi.org/10.1016/j.solener.2023.04.065.
[14] H. Du, et al., 24.18% efficiency TOPCon solar cells enabled by super hydrophilic carbon-doped polysilicon films combined with plated metal fingers, Sol. Energy Mater. Sol. Cell. 257 (2023), 112393, https://doi.org/10.1016/j.solmat.2023.112393.
[15] N. Mingirulli, et al., Interdigitated back-contacted silicon heterojunction solar cells with improved fill-factor and efficiency, in: 2011 37th IEEE Photovoltaic Specialists Conference, 2011, https://doi.org/10.1109/PVSC.2011.6186658.
[16] F. Feldmann, et al., Efficient carrier-selective p- and n-contacts for Si solar cells, Sol. Energy Mater. Sol. Cell. 131 (2014) 100–104, https://doi.org/10.1016/j.solmat.2014.05.039.
[17] W. Liu, et al., Polysilicon passivating contacts for silicon solar cells: interface passivation and carrier transport mechanism, ACS Appl. Energy Mater. 2 (7) (2019) 4609–4617, https://doi.org/10.1021/acsaem.8b02149.
[18] H. Shihua, et al., Simulation of silicon solar cells with passivation contact of tunnel oxide layer, Surf. Eng. Appl. Electrochem. 57 (5) (2021) 607–615, https://doi.org/10.3103/S1068375521050045.
[19] J. Huang, et al., Characterization of trap states distribution in poly-Si TFTs using OEMS, in: 2010 Symposium on Photonics and Optoelectronics, 2010, https://doi.org/10.1109/SOPO.2010.5504394.
[20] T. Watanabe, et al., Electrical properties of solid-phase crystallized polycrystalline silicon films, Appl. Phys. A 77 (1) (2003) 87–92, https://doi.org/10.1007/s00339-002-1513-6.
[21] J.J. Thevaril, S.K. O'Leary, Defect absorption and optical transitions in hydrogenated amorphous silicon, Solid states Communications 150 (37) (2010) 1851–1855, https://doi.org/10.1016/j.ssc.2010.06.034.
[22] C.Y. Chen, et al., Analysis of negative bias temperature instability in body-tied low-temperature polycrystalline silicon thin-film transistors, IEEE Electron. Device Lett. 29 (2) (2008) 165–167, https://doi.org/10.1109/LED.2007.914083.
[23] G.A. Armstrong, J.R. Ayres, S.D. Brotherton, Numerical simulation of transient emission from deep level traps in polysilicon thin film transistors, in: ESSDERC '96: Proceedings of the 26th European Solid States Device Research Conference, 1996, https://doi.org/10.1016/S0038-1101(97)00053-1.
[24] H. Sehil, et al., Characterization of the polysilicon thin film transistors elaborated in high and low temperature processes. Study of the density of traps, Synth. Met. 90 (1997) 181–185, https://doi.org/10.1016/S0379-6779(98)80004-0.
[25] K.-J. Kim, et al., A new charge pumping model considering bulk trap states in polysilicon thin film transistor, Solid-states Electronics 42 (1998) 1897–1903, https://doi.org/10.1016/S0038-1101(98)00156-7.
[26] W.B. Jackson, N.M. Johnson, D. Biegelsen, Density of gap states of silicon grain boundaries determined by optical absorption, Appl. Phys. Lett. 43 (1983) 195–197, https://doi.org/10.1063/1.94278.
[27] W.B. Jackson, et al., Hydrogen diffusion in polycrystalline silicon thin films, Appl. Phys. Lett. 61 (1992) 1670–1672, https://doi.org/10.1063/1.108446.
[28] N.A. Hastas, et al., Determination of interface and bulk traps in the subthreshold region of polycrystalline silicon thin-film transistors, IEEE Trans. Electron. Dev. 50 (2003) 1991–1994, https://doi.org/10.1109/TED.2003.815372.
[29] C.A. Dimitriadis, et al., Determination of bulk states and interface states distributions in polycrystalline silicon thin-film transistors, J. Appl. Phys. 74 (1993) 2919–2924, https://doi.org/10.1063/1.354648.
[30] Y. Jeong, et al., Effects of various hydrogenation processes on bias-stress-induced degradation in p-channel polysilicon thin film transistors, Jpn. J. Appl. Phys. 41 (2002) 5048, https://doi.org/10.1143/JJAP.41.5048.
[31] C.-H. Ling, C.Y. Kwok, T.M. Tay, Quasi-Fermi level variation in the space-charge region of a grain boundary, J. Phys. D 18 (1985) 671–675, https://doi.org/10.1088/0022-3727/18/4/011.